17th World Conference on Earthquake Engineering, 17WCEE
Sendai, Japan - September 13th to 18th 2020

EXPERIMENTAL STUDY ON THE IN-PLANE FLEXURAL BEHAVIOR OF CONFINED MASONRY WALLS

J. Varela-Rivera[(1)], L. Fernandez-Baqueiro[(2)], J. Moreno-Herrera[(3)]

[(1)] *Professor, Universidad Autonoma de Yucatan, vrivera@correo.uady.mx*
[(2)] *Professor, Universidad Autonoma de Yucatan, luis.fernandez@correo.uady.mx*
[(3)] *Associate Professor, Universidad Autonoma de Yucatan, joel.moreno@correo.uady.mx*

Abstract

The shear behavior of confined masonry walls has been widely studied by many authors. Variables studied were the unit type, types and quantities of steel reinforcement in confining elements, wall aspect ratio, openings and axial compressive stress, among others. In contrast, the flexural behavior of confined walls has been scarcely studied, the authors only found a single study on this type of behavior. In this paper, results of a study on the flexural behavior of confined masonry walls are presented. Six full-scale walls were tested in the laboratory under constant axial loads and reverse cyclic lateral loads until failure. The variables studied were the aspect ratio and the axial compressive stress of walls. Based on the experimental results it was observed that the flexural behavior of walls was in general similar. The behavior was characterized by horizontal flexural cracks followed by yielding of the longitudinal steel reinforcement of vertical confining elements. After this, vertical cracks were observed on the masonry panels. These cracks were associated with the brick bond pattern used in construction and the non-uniform vertical deformation on the walls. Vertical cracks caused a reduction in the shear strength of the walls. Because of this reduction, diagonal shear cracks were observed on the masonry panels. Failure of walls was associated with crushing of concrete at the bottom ends of the vertical confining elements. As expected, flexural strength of walls increased as the aspect ratio decreased, or the axial compressive stress increased. Flexural strength of walls was well predicted using flexural theory (kinematics, constitutive models and equilibrium). A displacement ductility capacity of 6 and a drift ratio capacity of 1% are proposed for the walls studied. For a displacement ductility at first yielding of 6, the normalized stiffness degradation of wall was about 20%. For a drift ratio of 1%, the normalized stiffness degradation of walls varied from 9% to 33%.

Keywords: confined masonry walls; flexural behavior; in-plane loads

1. Introduction

In many countries of Latin America, central and south Asia, and eastern and southern Europe, confined masonry walls are widely used as a structural system [1, 2]. Confined masonry consists of an unreinforced masonry panel with flexible reinforced concrete confining elements around its perimeter. In this type of construction, the masonry panel is constructed first and later the confining elements are concrete cast. The use of confined walls in Mexico is very common because of their low construction cost and ease of construction.

The shear behavior of confined walls under in-plane lateral loads has been widely studied. There are several experimental studies carried out by different authors. Main variables studied are the unit type [3, 4], combination of clay and concrete units [1], types and quantities of steel reinforcement in confining elements [5, 6], wall axial load [7, 8], wall aspect ratio (height over length) [8, 9, 10], toothing [11], wall openings and type of reinforcement around openings [12]. In general, these studies considered the shear behavior of confined walls with aspect ratios smaller than or equal to one. Only one study considered wall aspect ratios up to 2.2 [10]. Walls considered by those authors were constructed using clay or concrete units. The shear behavior of walls was characterized by diagonal cracks that eventually formed the traditional "X" final cracking pattern. Failure of walls was mainly associated with propagation of diagonal cracks into the top and bottom ends of vertical confining elements. Shear strength of walls was associated with the formation of the first diagonal crack. It was observed that confining elements increased the loading and deformation capacity of walls after reaching their shear strength.

In contrast, the flexural behavior of full-scale confined walls under in-plane lateral loads has been scarcely studied. The authors only found a study on the flexural behavior of a half-scale structure tested in a shaking table [13]. The structure consisted of two confined masonry walls with a reduced amount of flexural reinforcement. The behavior of the structure was dominated by the flexural behavior of the walls. There are some studies related to the in-plane flexural behavior of other types of masonry walls. In the case of reinforced walls, the main variables that have been studied are the quantity and distribution of reinforcement [14, 15], wall axial load [15, 16, 17] and wall aspect ratio [16, 17]. Flexural behavior of those walls was, in general, characterized by flexural cracks over the wall height followed by yielding of the longitudinal steel reinforcement. Failure of walls was mainly associated with crushing of the masonry or the concrete at wall ends. Flexural strength of walls was maintained over a certain maximum displacement ductility.

The objective of this paper is to study the flexural behavior of confined walls subjected to reverse cyclic loads. Results of six confined walls subjected to lateral loads are presented. The variables studied were the wall aspect ratio and the wall axial compressive stress. The final cracking patterns of walls are presented. The lateral load – drift ratio curves for the walls are analyzed. A discussion related with flexural strength, displacement ductility and drift ratios is presented.

2. Experimental program

Six full-scale confined walls were tested in the laboratory (walls M1 to M6). Walls were constructed using hollow clay bricks with nominal dimensions of 115 mm × 200 mm × 320 mm (thickness × height × length). The ratio between net and gross area of the bricks was about 0.54. The study variables were the wall aspect ratio (H/L) and the axial compressive stress (σ) (Table 1). Aspect ratios were selected to be greater than one (1.1, 1.5 and 2.4) to facilitate wall flexural behavior. Axial compressive stresses of 0.24 MPa, 0.47 MPa and 0.72 MPa corresponded to two, four and six-story masonry structures, respectively. The amount of vertical reinforcement was selected to induce flexural behavior. Details of each confined wall are presented in Table 1. In this table, H, L and t are the wall height, length and thickness, respectively. The wall height was measured up to the point of load application.

Table 1 – Details of confined walls

Wall	H (m)	L (m)	t (mm)	H/L	σ (MPa)	ρ (%)
1	2.91	2.54	115	1.1	0.24	0.024
M2	2.91	1.88	115	1.5	0.24	0.033
M3	2.91	1.88	115	1.5	0.47	0.033
M4	2.91	1.22	115	2.4	0.24	0.051
M5	2.91	1.22	115	2.4	0.47	0.051
M6	2.91	1.22	115	2.4	0.71	0.051

Cross-section dimensions of vertical confining elements were 115 mm × 115 mm (width × height). Longitudinal steel reinforcement in those elements consisted of a 1#3 (9.5 mm) bar (Fig. 1). The corresponding steel reinforcement ratio (ρ) is included in Table 1. This ratio was calculated using the wall cross-section. No transverse reinforcement was placed on the vertical confining elements. Longitudinal reinforcement consisted of deformed steel bars with nominal yield strength of 412 MPa. The amount of longitudinal steel reinforcement of the walls was smaller than the minimum amount prescribed in the Mexico City Masonry Technical Norm [18]. Walls were constructed in half running bond by an experienced worker. Brick courses were laid using mortar in proportion by volume 1:3 (Portland cement: sand). Mortar was placed on both the face shells and the head joints. Average thickness of mortar joints was 10 mm.

The average compressive strength of concrete of walls M1 to M6 was equal to 17.49, 18.10, 20.00, 18.36, 22.16 and 21.23 MPa, respectively. Corresponding coefficient of variation (CV) was equal to 0.08, 0.04, 0.03, 0.08, 0.02 and 0.01, respectively. Average compressive strength of units was equal to 16.33 MPa with a CV of 0.06. Average compressive strength of mortar was equal to 15.85 MPa with a CV of 0.08. Average compressive strength and modulus of elasticity of masonry were equal to 9.08 and 5077 MPa, respectively. Corresponding CV was equal to 0.04 and 0.12, respectively. The average yielding strength of the longitudinal steel reinforcement was equal to 445.7 MPa with a CV of 0.02. All values were calculated using gross properties of corresponding cross-sections.

Each confined wall was tested with constant axial load and reverse monotonic cyclic lateral loads until failure. Axial load for each wall was calculated using the corresponding axial compressive stress, wall length and wall thickness (Table 1). Axial load was applied using a swivel beam, a spreader beam, two threaded rods and a hydraulic actuator (Fig. 1a). Pressure in the actuator was maintained constant during the test using a mechanical load maintainer [19]. Axial load was measured using two donut type load cells. This load was verified using a pressure transducer. Lateral loads were applied using a steel frame, a loading steel beam, and a two-way hydraulic actuator (Fig. 1b). Lateral load was measured using a tension-compression pin load cell. Wall specimens were attached to the lab reaction floor.

Horizontal and vertical wall displacements and shortening or lengthening of wall diagonals were measured using linear string potentiometers. Relative displacements between the loading beam and the wall, the wall and the wall foundation, and the wall foundation and the reaction floor were measured using linear potentiometers. Strain gages were attached to the longitudinal steel reinforcement of both vertical confining elements. Two strain gages were located at the bottom of each bar.

Loading history used to test the walls was based on the protocol established in the Mexico City Masonry Technical Norm [18]. This loading history has six initial reverse cycles controlled by load and subsequent cycles controlled by drift ratios. The maximum target load was associated with yielding of the longitudinal steel reinforcement of the vertical confining elements. The target load for the first two cycles was equal to one quarter of the maximum target load, the third and fourth cycles to one half of the maximum target load, and the fifth and sixth cycles to the maximum target load. After that, increments of drift ratios of 0.002 were applied.

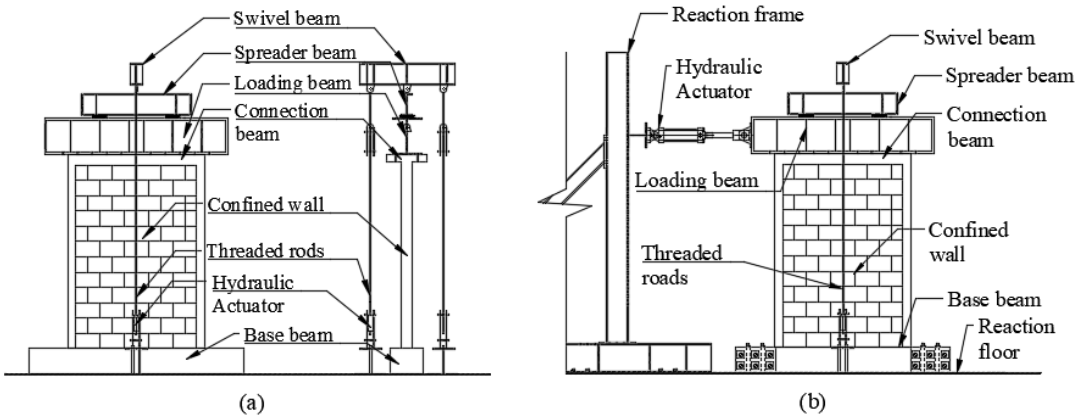

Fig. 1 – (a) axial load test setup, (b) lateral load test setup

3. Experimental results

The flexural behavior of walls was, in general, similar. First, a horizontal flexural crack was observed at the joint between the first brick course and the concrete foundation together with horizontal flexural cracks on the bottom part of the vertical confining elements. After this, yielding of the longitudinal steel reinforcement at the bottom end of the vertical confining element in tension was reached. As the drift ratio was increased, horizontal flexural cracks propagated into the masonry panel and new flexural cracks were observed along the height of the vertical confining elements. A single vertical crack was observed for walls M2, M4 and M5 and two vertical cracks for walls M3 and M6 (Fig. 2). Diagonal shear cracks were observed on the masonry panels. These cracks propagated from the top part of the masonry panels to the existing vertical cracks. Out-of-plane buckling of one of the vertical confining elements was observed for wall M5. Failure of walls was associated with crushing of concrete at the bottom part of the vertical confining elements. The final cracking patterns of walls are presented in Fig. 2. Lateral load – drift ratio curves of walls are presented in Fig. 3.

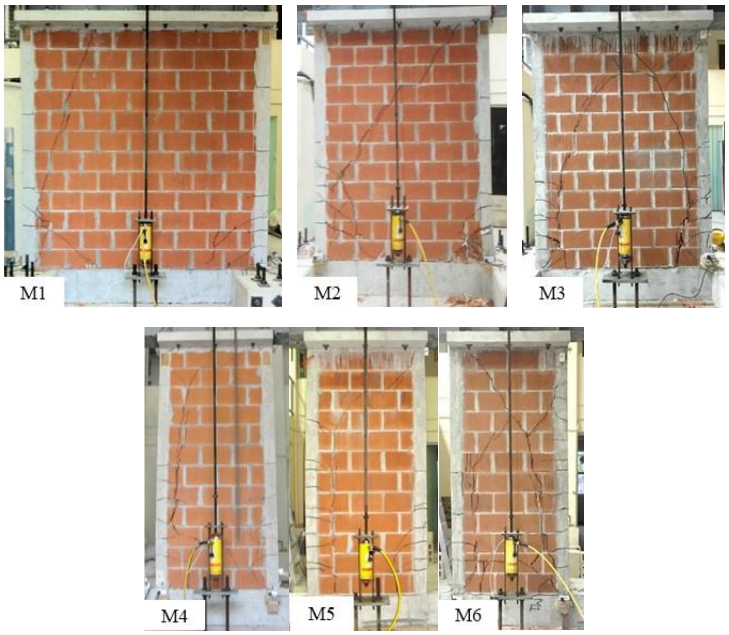

Fig. 2 – Final cracking patterns of walls

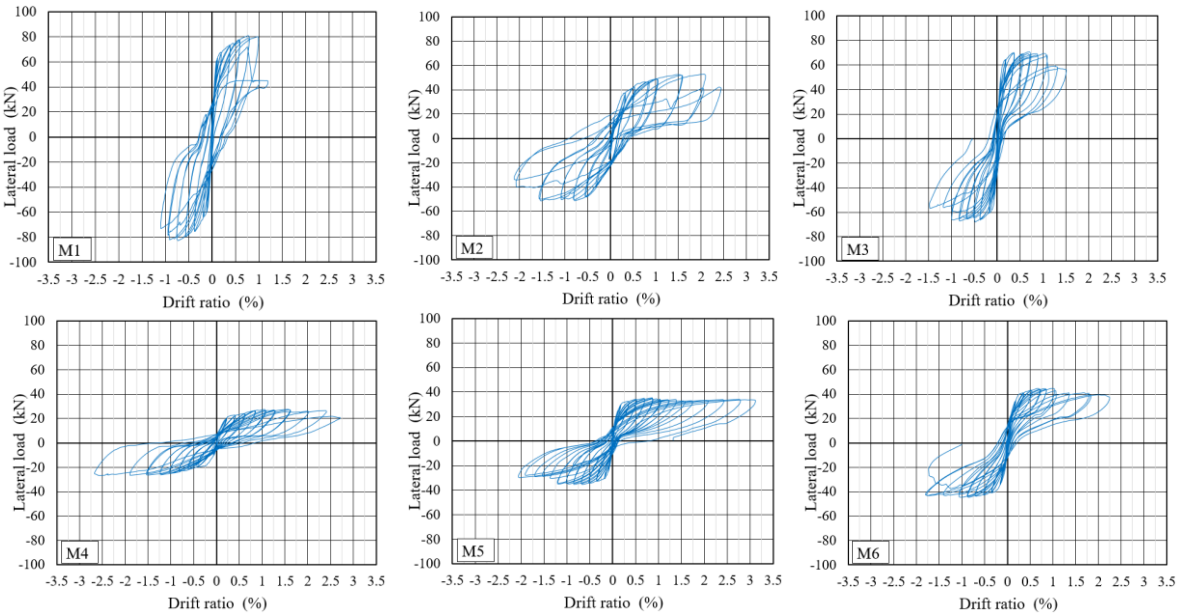

Fig. 3– Lateral load – drift ratio curves of walls

4. Discussion of results

The experimental average flexural strengths of walls (M_e) are presented in Table 2. These strengths were calculated using corresponding positive and negative maximum observed lateral loads. As expected, for walls with the same axial compressive stress (walls M1, M2 and M4), the flexural strength increased as the aspect ratio decreased (Fig. 4). For walls with the same aspect ratio (M4 to M6), the flexural strength increased as the axial compressive stress increased (Fig. 3). Analytical flexural strengths of walls (M_a) are also presented in Table 2. These strengths were calculated using flexural theory (kinematics, constitutive models and equilibrium). A rectangular block was used for the compressive stresses of concrete [20]. This type of block was used because the wall neutral axis was located within the height of the vertical confining element. A stress-strain relationship of the steel including strain hardening was used [21]. A good agreement between analytical and experimental flexural strengths (M_a/M_e) was observed for the walls (Table 2). The ratio M_a/M_e varied from 0.98 to 1.06.

Maximum horizontal displacements were calculated for the walls, one in each loading direction. These displacements were limited by a 10% strength degradation or the presence of the first diagonal crack on the wall, whichever happened first. A value of displacement capacity (d_m) (Table 2) was proposed for each wall as the minimum between the maximum horizontal displacements in the corresponding positive and negative loading directions.

Table 2 – Experimental and analytical flexural strengths, displacement ductilities and drift ratios of walls.

Wall	H/L	σ (MPa)	ρ (%)	M_e (kN-m)	M_a (kN-m)	d_m (mm)	d_{fy} (mm)	μ_{fy}	δ
M1	1.1	0.24	0.024	237.71	237.71	28.0	3.0	9.33	0.96
M2	1.5	0.24	0.033	151.82	158.37	51.5	3.6	14.31	1.77
M3	1.5	0.47	0.033	201.47	199.76	30.4	2.4	12.66	1.04
M4	2.4	0.24	0.051	79.33	83.90	70.0	7.9	8.86	2.41
M5	2.4	0.47	0.051	102.73	104.16	40.0	5.2	7.69	1.37
M6	2.4	0.71	0.051	130.13	126.99	30.3	5.0	6.06	1.04

Drift ratios were calculated dividing the displacement capacities (d_m) (Table 2) by the wall height (H) (Table 1). Wall drift ratios (δ) are presented in Table 2. Displacement ductility is defined as the ratio of a maximum displacement to a given yielding displacement. Maximum displacements of the walls were defined as the displacement capacities (d_m) (Table 2). Yielding displacements were calculated using the average strain readings of 0.0022 (d_{fy}) (Table 2). This displacement is associated with first yielding of the steel reinforcement of the vertical confining elements. Displacement ductilities at first yielding (μ_{fy}) are presented in Table 2. For walls with the same axial compressive stress (walls M1, M2 and M4), drift ratio increased as the wall aspect ratio increased. Corresponding displacement ductilities (μ_{fy}) did not follow that trend because walls M1, M2 and M4, with the same axial compressive stress, had different axial loads (P) (Table 2) and different steel reinforcement ratios (ρ) (Table 2). Displacement ductility (μ_{fy}) increases as the axial load decreases or the steel reinforcement ratio decreases. Wall M1 had the maximum axial load but the minimum steel reinforcement ratio. Wall M4 had the minimum axial load but maximum steel reinforcement ratio. For walls with the same aspect ratio (walls M4 to M6), as expected, drift ratios (δ) and displacement ductilities (μ_{fy}) increased as the axial compressive stress decreased. The displacement ductilities (μ_{fy}) of the walls varied from 6.06 to 14.31. The drift ratios (δ) varied from 0.96% to 2.41%. These values showed that the confined walls studied had a good deformation capacity under lateral loads. The minimum displacement ductility (μ_{fy}) and drift ratio (δ) of the walls were about 6 and 1%, respectively. Based on those minimum values, a displacement ductility capacity of 6 and a drift ratio capacity of 1% are proposed for the confined walls studied.

Vertical cracks were observed for walls M2 to M6, one for walls M2, M4 and M5 and two for walls M3 and M6. For walls M3 to M6 the first vertical crack was observed after the corresponding flexural strength. For wall M2 the vertical crack was observed first. Vertical cracks formed on the wall side in compression. These cracks were, in general, located on the bottom brick courses at about 150 mm from the joint between the vertical confining elements and the masonry panel (Fig. 2). Vertical cracks were associated with the brick bond pattern used in construction and the non-uniform vertical deformation along the wall length. The mortar head joints of alternating end bricks were vertically aligned (Fig.2). It was observed during testing that vertical cracks formed first at those head joints and then propagated into the bricks. This was related to the smaller compressive strength of the mortar of joints compared with that of the bricks. The non-uniform vertical deformation along the wall length was caused by the difference between the modulus of elasticity of concrete and masonry. The modular ratio between concrete and masonry was about 3. For example, under only axial load, the axial stress on the wall is uniform but the bricks close to the vertical confining elements tend to deform less than those located at the wall midlength. This deformation gradient was greater for the walls with the smaller length. Wall M1 with the largest length did not have any vertical crack. Under lateral loads, the compressive stress increases at the corresponding wall end. Vertical cracks divided the walls into wall segments. As the "effective" wall length decreased, the shear strength of the walls also decreased. This strength reduction triggered the formation of the diagonal cracks observed on the walls.

The secant stiffness at yielding of the steel longitudinal reinforcement (K_y) of the walls M1 to M6 was equal to 19959, 8463, 21772, 2737, 5574, and 6775 kN/m, respectively. Each yielding stiffness was calculated using the displacements at first yielding (d_{fy}) and only the first positive cycles. For walls with the same axial stress (walls M1, M2 and M4), the secant yielding stiffness decreased as the aspect ratio increased. For walls with the same aspect ratio (walls M4, M5 and M6), the secant yielding stiffness increased as the axial stress increased. Normalized stiffness degradation (K_i/K_y) curves for the walls as a function of the displacement ductility (μ_{fy}) and drift ratio are presented in Figures 4a and 4b, respectively. The secant stiffness (K_i) of each positive cycle was divided by the secant yielding stiffness (K_y). Load cycles up to the values of displacement capacities of walls (d_m) (Table 2) were included.

For a given displacement ductility (μ_{fy}), the normalized stiffness degradation of walls was similar (Fig. 4a). For displacement ductilities (μ_{fy}) of 2, 4, and 6, the normalized stiffness degradation was about 55%, 30%, and 20%, respectively. For a given drift ratio, the stiffness degradation of walls was different (Fig. 4b). For a drift ratio of 0.5% and 1%, the normalized stiffness degradation varied from 18% to 60% and 9% to 33%, respectively. The relationship between displacement ductilities (μ_{fy}) and corresponding drift ratios of

walls are presented in Fig. 4c. For walls M1, M2, M3, M5 and M6, the displacement ductility capacity of 6 is reached before the drift ratio capacity of 1%. For wall M4, with the smallest secant stiffness at yielding, the drift ratio capacity of 1% is reached first.

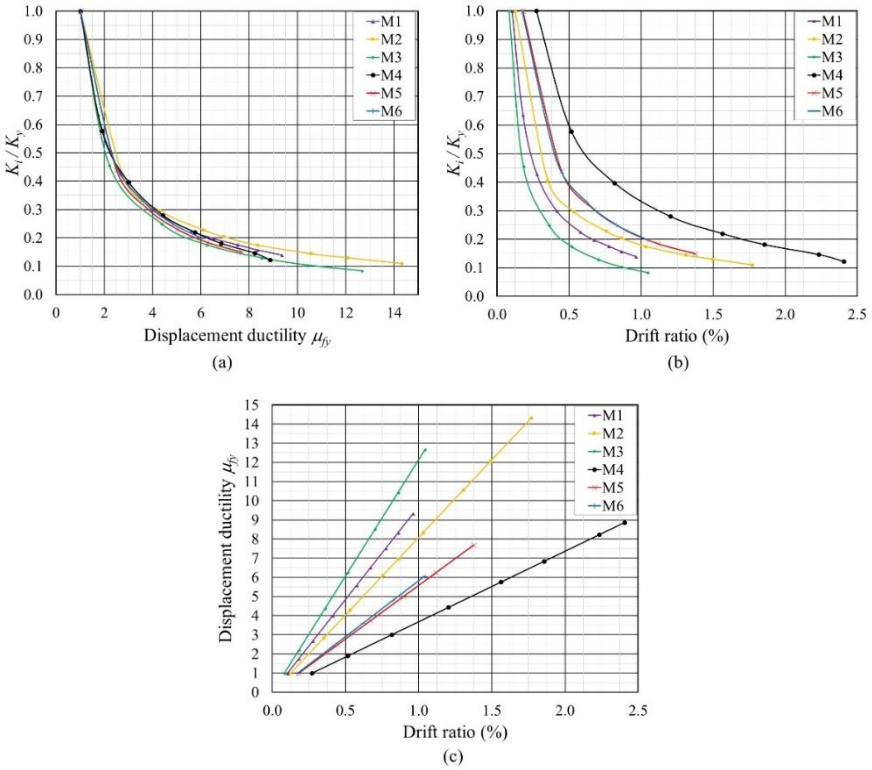

Fig.4 – (a) Normalized stiffness degradation as a function of displacement ductility, (b) normalized stiffness degradation as a function of drift ratio and (c) relationship between displacement ductility and drift ratio of walls.

5. Conclusions

Six confined masonry walls with aspect ratios greater than one were tested in the laboratory under reverse cyclic lateral loads. Walls were designed to induce flexural behavior. Based on the results obtained in this work, the following conclusions are presented:

- Flexural behavior of walls was characterized by yielding of the longitudinal steel reinforcement followed by vertical and diagonal cracks. Failure of walls was associated with crushing of concrete at the bottom ends of vertical confining elements. As expected, flexural strength of walls increased as the aspect ratio decreased, or the axial compressive stress increased. Flexural strength of walls can be determined using flexural theory (kinematics, constitutive models and equilibrium).
- The confined walls studied had a good deformation capacity under lateral loads. The displacement ductilities at first yielding varied from 6.06 to 14.31 and the drift ratios from 0.96% to 2.41%. Based on the observed minimum values, a displacement ductility capacity of 6 and a drift ratio capacity of 1% are proposed for the walls. For a displacement ductility at first yielding of 6, the normalized stiffness degradation of wall was about 20%. For a drift ratio of 1%, the normalized stiffness degradation of walls varied from 9% to 33%.
- The vertical cracks observed on the walls caused a reduction in their shear strength. Because of this reduction, diagonal shear cracks were observed in the walls. Vertical cracks were associated with the brick bond pattern used in construction and the non-uniform vertical deformation on the wall.

6. References

[1] Tena-Colunga, A., Juárez-Ángeles A., and Salinas-Vallejos, V. H. (2009): Cyclic Behavior of Combined and Confined Masonry Walls, *Engineering Structures*, 31:1, 240-259.

[2] Riahi, Z., Elwood, K., and Alcocer, S. M. (2009): Backbone Model for Confined Masonry Walls for Performance Based Seismic Design, *Journal of Structural Engineering*, 125:6, 644-654.

[3] Meli, R. (1979): *Comportamiento Sísmico de Muros de Mampostería, Tech. Rep. Serie Azul: Instituto de Ingeniería, UNAM, No. 352*, Mexico City, Mexico. [in Spanish]

[4] San Bartolome, A., and Quiun, D. (2010): Diseño Sísmico de Edificaciones de Albañilería Confinada, *Revista Ciencia*, Mexico City, Mexico, 13:2, 161-185. [in Spanish]

[5] Treviño, E. L., Alcocer, S. M., Flores, L. E., Larrua, R., Zarate, J. M., and Gallegos, L. (2004): Investigación Experimental del Comportamiento de Muros de Mampostería Confinada de Bloques de Concreto Sometidos a Cargas Laterales Cíclicas Reversibles Reforzados con Acero de Grados 60 y 42, *In Proceedings, XIV Congreso Nacional de Ingeniería Estructural*, October, 2004, Acapulco, Mexico. [in Spanish]

[6] Quiroz, L., Maruyama, Y., and Zavala, C. (2014): Cyclic Behavior of Peruvian Confined Masonry Walls and Calibration of Numerical Model Using Genetic Algorithms, *Journal of Engineering Structures*, 75, 561-576.

[7] Urzua, D. A., Padilla, M. R., and Loza, J. R. (2001): Influencia de la Carga Vertical en la Resistencia Sísmica de Muros de Mampostería Confinada con Materiales Pumíticos Típicos de Guadalajara, *In Proceedings, XIII Congreso Nacional de Ingeniería Sísmica*, October 2001, Guadalajara, Mexico. [in Spanish]

[8] Castilla E., and Marinilli A. (2000): Recent Experiments with Confined Concrete Block Masonry Walls, *In Proceedings of 12th International Brick/Block Masonry Conference*, 2000, Madrid, Spain.

[9] San Bartolomé, A., Quiun, D., and Torrealva, D. (1992): Seismic Behaviour of a Three-Story Half Scale Confined Masonry Structure, *In Proceedings of Earthquake Engineering, Tenth World Conference*, 1992, Balkema, Rotterdam.

[10] Perez Gavilan, J. J., Flores, L. E., and Alcocer, S. M. (2015): An Experimental Study of Confined Masonry Walls with Varying Aspect Ratio, *Earthquake Spectra*, 31:2, 945-968.

[11] Singhal V. and Rai D.C. (2016): In-plane and out-of-plane Behavior of Confined Masonry Walls for Various Toothing and Opening Details and Prediction of their Strength and Stiffness, *Earthquake Engineering, Structural Dynamics*, 45:15, 2551-2569.

[12] Flores, L. E., Mendoza J. A., and Reyes C. (2004): Ensaye de Muros de Mampostería con y sin Refuerzo Alrededor de la Abertura, *In Proceedings, XIV Congreso Nacional de Ingeniería Estructural*, October, 2004, Acapulco, Mexico. [in Spanish]

[13] Bustos J.L., Zavala F., Masanet A.R. and Santalucía J.R. (2000): Estudio del Comportamiento Dinámico de un Modelo de Mampostería Encadenada Mediante un Ensayo en mesa Vibratoria, *In Proceedings, XXIX Jornadas Sudamericanas de Ingeniería Estructural*, November, 2000, Punta del Este, Uruguay. [in Spanish]

[14] Yoshimura, K., Kikuchi, K., Kuroki, M., Liu, L., and Ma, L. (2000): Effect of wall reinforcements, applied lateral forces and vertical axial loads on seismic behavior of confined concrete masonry walls, *In Proceedings of the 12 World Conference on Earthquake Engineering*, 30-January to 4-February, 2000, Auckland, New Zealand.

[15] Shedid, M. T., Drysdale, R. G., El-Dakhakhni, W. W. (2008): Behavior of Fully Grouted Reinforced Concrete Masonry Shear Walls Failing in Flexure: Experimental Results, *Journal of Structural Engineering*, ASCE, 134:11, 1754-1767.

[16] Tanner, J. E., Varela, J. L., Klinger, R. E., and Brightman, M. J. (2005): Seismic Testing of Autoclaved Aerated Concrete Shear-Walls: A Comprehensive Review, *ACI Structural Journal*, 102:3, 374-382.

[17] Varela, J. L., Tanner, J. E., and Klinger, R. E. (2006): Development of Seismic Force Reduction and Displacement Amplification Factors for Autoclaved Aerated Concrete Structures, *Earthquake Spectra*, 22:1, 267-286.

[18] NTC-M (2004): Normas Técnicas Complementarias para Diseño y Construcción de Estructuras de Mampostería, Reglamento de Construcciones para el Distrito Federal, Gaceta Oficial del Distrito Federal, October 2004, Mexico City, Mexico. [in Spanish]

[19] Edison, 1994. Edison hydraulic Load Maintainers, Operation and Maintenance Manual. *Edison hydraulic load maintainers*, Paradise, California, USA. http://edisonhlm.com

[20] NTC-C (2004): Normas Técnicas Complementarias para el Diseño y Construcción de Estructuras de Concreto, Reglamento de Construcciones para el Distrito Federal, Gaceta Oficial del Distrito Federal, October 2004, Mexico City, Mexico. [in Spanish]

[21] Rodríguez, M., and Botero, J. C. (1997): Evaluación del Comportamiento de Barras de Acero de Refuerzo Sometidas a cargas Monotónicas y Cíclicas Reversibles Incluyendo Pandeo, *Revista de Ingeniería Sísmica*, 56, 9-27. [in Spanish]

